GAMANAM- Global **A**dvances in **M**ultidisciplinary **A**pplications in **N**ext-Gen **A**nd **M**odern Technologies
Volume 1, Issue 2, April 2025

Research Paper

An Optimized Edge Preserving Medical Image Fusion Framework Using NSCT for Improved Diagnostic Accuracy

[1*] B.Nagasirisha, [2] G.Vijay Kumar Reddy, [3] K.Sugunamma, [4] G.Abhishek, [5] K Sai Teja

SR Gudlavalleru Engineering College,Gudlavalleru, Andhra Pradesh, India

**Corresponding Author(s):* nagasirishab@gmail.com

Received: 21/01/2025 Revised: 26/02/2025 Accepted: 15/03/2025 Published: 01/04/2025

Abstract: Medical image fusion plays a crucial role in enhancing diagnostic accuracy by integrating complementary information from multiple imaging modalities. This study presents an optimized fusion framework that combines Contrast Limited Adaptive Histogram Equalization (CLAHE) for image enhancement, Non-Subsampled Contourlet Transform (NSCT) for multi-scale decomposition, guided filtering for edge preservation, and gradient-based weight computation for detail layer fusion. The proposed method effectively preserves critical structural details while minimizing information loss and fusion artifacts. Experimental results demonstrate that the method achieves a minimum improvement of 5.75% and a maximum improvement of 38.23% in information retention, while fusion loss is reduced by 6.09% to 79.52%, and fusion artifacts are minimized by 10.00% to 96.97% compared to traditional approaches. The fused images exhibit superior visual quality, enhanced contrast, and improved feature preservation, making the method highly suitable for medical diagnosis and treatment planning.

Keywords*:* Medical image fusion, Contrast Limited Adaptive Histogram Equalization, Non-Subsampled Contourlet Transform, visual quality, medical diagnosis and treatment planning

---

1. Introduction

For a number of reasons, such as research, monitoring, precise illness diagnosis, and treatment planning, radiologists and other medical practitioners need images with great spatial and spectral resolution. Nevertheless, a single imaging modality sometimes falls short of offering complete information. For example, magnetic resonance imaging (MRI) is a better way to collect details about soft tissues than computed tomography (CT) images, which are more effective at highlighting bone structures. Similar to this, functional information is provided by positron emission tomography (PET) pictures, however they frequently lack accurate border features. Integrating data from several imaging modalities is crucial to overcoming these constraints. The process of image fusion creates a single, improved image with more diagnostic value by combining complimentary data from several imaging sources, including CT, MRI, and PET. In order to ensure that the fused image contains more significant information than any single source image, the technique pulls pertinent data from numerous input images. Applications of image fusion are found in many different domains, such as multi-focus image fusion, robotics, medical imaging, and satellite and aerial imaging [1-2].

There are various levels at which the fusion process might happen: To preserve as much detail as possible, pixel-level fusion keeps a large portion of the original images' raw data. Different properties, including borders and textures, from several photos are combined in feature-level fusion. To reach a final judgment, decision-level fusion integrates the information that has been processed. Image fusion can be divided into two main categories: single-sensor fusion, which combines pictures taken under diverse circumstances (such as multiple focus or exposure), and multi-sensor fusion, which combines images from various sensors and is frequently employed in defense and medical imaging applications. In clinical settings, medical image fusion is essential, especially for diagnosis and therapy planning. It makes use of cutting-edge methods from artificial intelligence, machine learning, image processing, computer vision, and pattern recognition. Numerous medical imaging technologies offer distinct benefits, including nuclear magnetic resonance (NMR) spectroscopy, CT, MRI, PET, Single Photon Emission

Computed Tomography (SPECT), Magnetic Resonance Angiography (MRA), and Ultrasonography (USG). Functional imaging techniques like PET, SPECT, and functional MRI (fMRI) offer important physiological insights, while structural imaging techniques like CT, MRI, and MRA provide high-resolution anatomical details[3-6].

Medical image fusion combines anatomical and functional imaging to create a single fused image from many input images, improving diagnosis accuracy, reducing redundant information, and lowering storage costs. For instance, by utilizing the advantages of both modalities, combining CT and MRI scans enhances the detection of anomalies. Similar to this, PET/MRI fusion helps with clinical diagnosis and treatment planning by integrating structural and functional data. Several important factors need to be taken into mind when using picture fusion techniques: All pertinent information from the initial images should be retained during the fusion process. Inconsistencies or artifacts added during fusion shouldn't deceive future image analysis or human viewers. The fusion technique should be reliable, consistent, and able to deal with missing data, noise, and registration problems. Medical imaging includes a variety of scan types, including CT, MRI, PET, and SPECT scans, all of which are essential for effectively identifying and evaluating patient diseases. These imaging modalities can be integrated using fusion techniques to produce a more thorough and insightful image, which will ultimately enhance clinical decision-making [7-8].

2. Literature review

Over the past few decades, numerous image fusion techniques have been introduced. For medical image integration, Agarwal et al. [9] proposed a hybrid method that merges wavelet transform (WT) and curvelet transform (CVT). In this approach, segmented input images undergo fusion in sub-bands using WT, while CVT divides these bands into overlapping tiles, effectively converting curves into straight lines. To achieve a more comprehensive fusion result, the tiles are blended using the inverse wavelet transform. The results indicate that this fusion strategy enhances image quality while reducing errors. Another advanced hybrid technique has been developed for multi-focus image fusion, combining principal component analysis (PCA) with stationary wavelet transform (SWT) [10]. SWT decomposes the final image into four sub-bands, capturing features from both the source and fused images. The PCA-based fusion algorithm is then applied to determine the most significant eigenvector for each sub-band, ensuring optimal image representation. By enhancing image information and reducing artifacts, this technique contributes to improved visual perception, as indicated by evaluation metrics.

Bavirisetti & Dhuli [11] introduced an edge-preserving fusion method tailored for visible and infrared sensor images, aiming to enhance image quality while minimizing artifacts. Their approach utilizes anisotropic diffusion to separate source images into approximation and detail layers. The final fused image is computed using the Karhunen-Loeve transform and linear superposition of these layers, significantly improving contrast while preserving essential image details. To address limitations in conventional fusion methods, a multiscale fusion framework based on weighted least squares (WLS) optimization and visual saliency maps (VSM) was introduced [12]. This method decomposes input images into basic and detail layers using a multiscale filtering technique that integrates Gaussian and rolling guidance filters (RGF). It effectively reduces halo artifacts while preserving scale-specific features, leading to a more visually natural fusion output.

Another fusion framework, designed for multimodal images, employs fast spatial filtering [13]. It begins by assessing an image's sharpness and contrast using gradient magnitude. A morphological closing operation is then applied to refine structures by filling gaps. The gradient magnitude is subsequently transformed into a weight map using a structure-preserving filter, and a weighted sum rule is applied to generate the final fusion result. This method enhances realism in multimodal images. Several coupled fusion image techniques have been explored, such as coupled image factorization optimization and a modified flexible coupling approach [14], is focusing on matrix and tensor factorization optimization. Experimental results suggest that the CIF-OPT approach performs well in noisy conditions, allowing precise image reconstruction without compromising critical features. Earlier methods often suffered from issues like color distortion, blurring, and noise.

To address these challenges, a Laplacian re-decomposition (LRD) technique was proposed for multimodal medical image fusion [15]. This method integrates two key advancements: a Laplacian decision graph decomposition strategy, which enhances images by providing complementary and redundant details, and an overlapping and non-overlapping domain approach to manage different types of information. Goyal et al. [16] recently introduced a multimodal medical image fusion method designed to integrate low-resolution medical images with minimal computational complexity, improving target recognition accuracy for clinical applications. Similarly, Jose et al. [17] developed a multimodal approach using the Non-Subsampled Shearlet Transform (NSST) for applications in identity search. NSST, a multi-scale and multi-directional wavelet transform, has also been employed by Kaur and Singh [18] in a medical image fusion method that segments images into sub-bands. Features from input images are extracted using an advanced inception model, and decisions are optimized via multi-objective differential evolution. The fusion process leverages coefficients of determination and energy loss to generate the final fused image using an inverse NSCT. Additionally, Srikanth et al. [19-22] explored brain tumor identification through image fusion by employing metaheuristic algorithms. Their study presents a fusion framework utilizing cross-guided filters and convolutional neural networks (CNNs) to enhance medical image analysis.

3. Proposed methodology

The proposed fusion mechanism integrates CT and MRI images using an advanced multi-stage approach to enhance medical image clarity. Initially, both images undergo

Contrast-Limited Adaptive Histogram Equalization (CLAHE) for enhancement, improving local contrast. Next, Non-Subsampled Contourlet Transform (NSCT) decomposes each image into base and detail layers. The base layers, which contain low-frequency information, are fused using an energy-based fusion technique to preserve structural details. Meanwhile, the detail layers, carrying high-frequency edge information, undergo further processing via a guided filter, which enhances edge preservation. The gradients of the filtered outputs are then used to compute a weight map, assigning fusion weights W1 and W2 for the detail layers. A weighted average fusion is applied to combine the detail layers effectively. Finally, the fused base and detail layers are reconstructed using inverse NSCT, generating the final fused image, which retains the structural clarity of CT scans and the soft tissue details of MRI scans for improved medical diagnosis. The process flow is illustrated in figure 1.

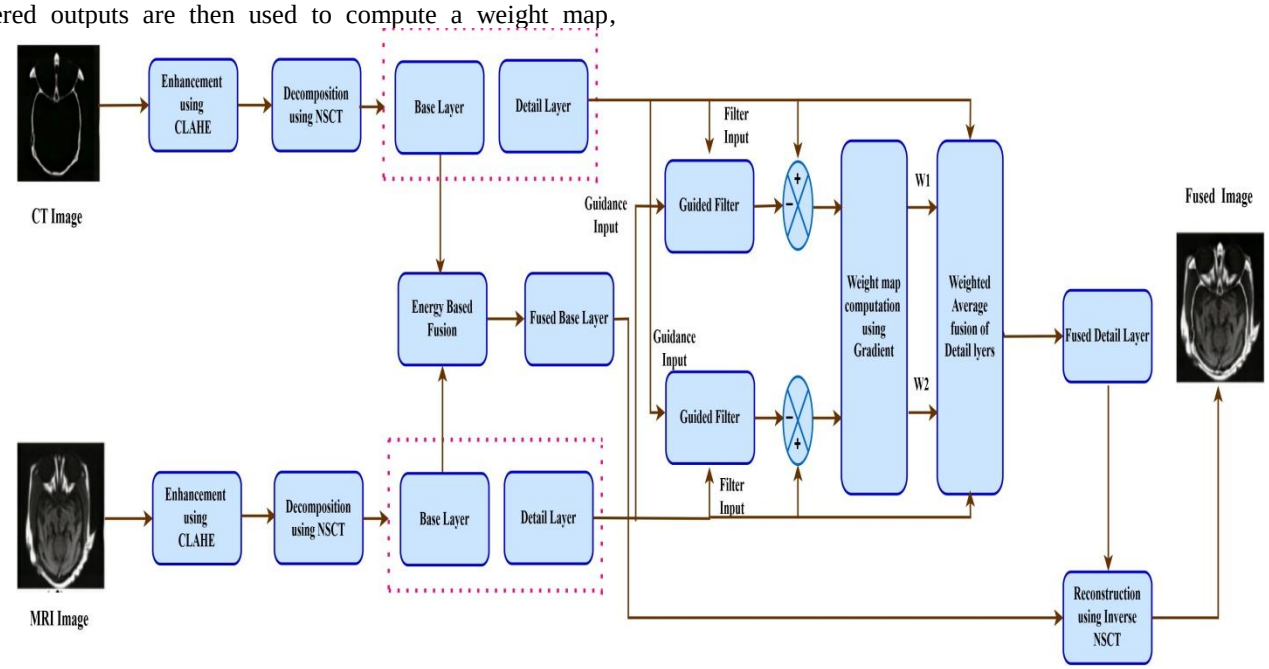

Figure 1: Process flow of proposed fusion mechanism

3.1 Image Enhancement using CLAHE

The primary objective of this step is to improve the contrast of CT and MRI images to enhance feature visibility before fusion. CLAHE operates on small contextual regions of an image, applying histogram equalization while limiting contrast amplification.

Given an image $I(x, y)$, CLAHE is applied as:

$$I_{CLAHE}(x, y) = HE(I(x, y)|_{clip\ limit} \quad (1)$$

Where HE denotes histogram equalization operation

.

clip limit is a predefined threshold that prevents over-enhancement.

Each of the source images is subjected to CLAHE operation. These contrast-enhanced images are then subjected to NSCT decomposition.

3.2 Multi-scale Decomposition using NSCT

In contrast to wavelets, NSCT is a multi-scale, multi-directional transform that preserves shift-invariance while capturing fine features and edge structures of an image. It has two primary phases called multiscale decomposition and multi-directional decomposition as shown in figure 2

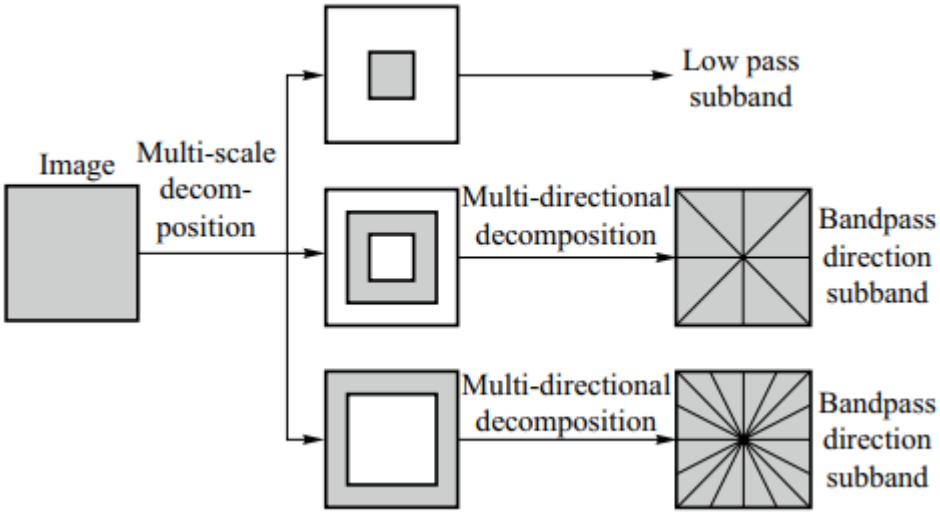

Figure 2: Image decomposition using NSCT

Non-Subsampled Pyramid (NSP): Decomposes the image into high-frequency (detail layers) and low-frequency (base layer) components. NSP uses iterative low-pass filtering to generate multiple frequency bands.

Low pass filtered image at scale 'l' is given as

$$B_l(x,y) = B_{l-1}(x,y) * h_{LPF}(x,y) \quad (2)$$

High pass filtered image at scale 'l' is given as $D_l(x,y) = B_{l-1}(x,y) - B_l(x,y)$ (3)

Where $h_{LPF}(x,y)$ is kernel of low pass filter and '$*'$ denotes convolution operation.

Non-Subsampled Directional Filter Bank (NSDFB): Decomposes high-frequency components into directional sub-bands at different scales.

The high-frequency components D_l through the Non-Subsampled Directional Filter Bank (NSDFB). This further decomposes them into k directional sub-bands.

$$D_{l,k}(x,y) = D_l(x,y) * h_{\theta_k}(x,y) \quad (4)$$

Where $h_{\theta_k}(x,y)$ are directional filter kernels at orientations θ_k and $D_{l,k}(x,y)$ is the detail component at scale l and direction k.

3.3 Energy of an Image: This works considers local energy of base layers for fusing them and criteria to compute local energy and then fusing base layers using energy based weight maps is as given below:

Let $W_c = \frac{1}{9}\begin{bmatrix}1 & 1 & 1\\ 1 & 1 & 1\\ 1 & 1 & 1\end{bmatrix}$ is a 3x3 window used to compute the smoothened coefficients of an image.

Then energy of an Image $B_l(x,y)$ is given as follows:

$$E(x,y) = \sum_p \sum_q [B_l(x+p, y+q)]^2 \, W_c(p,q) \quad (5)$$

3.4 Gradient computation of an image:

This work considers the guided filter output of a detail layer input to compute the gradient of an image. Guided filter is an edge preserving filter that mainly operates on four parameters called filtering input, guidance input, regularization parameter (ϵ) and radius (r). Radius is used to decide the size of the kernel for image smoothening operation according to the relation $N = 2r + 1$ while regularization parameter (ϵ) is used to decide whether the current pixel is edge pixel or non-edge pixel. Guidance input can be same as filtering input. If guidance input for filtering first image is taken from second image and vice-versa then the filter can be named as cross guided filter. More information on guided filter can be found at [23]

For an image P, gradient can be computed as $G = \sqrt{\left(\frac{\partial P}{\partial x}\right)^2 + \left(\frac{\partial P}{\partial y}\right)^2}$ (6)

3.5 Algorithm of proposed fusion mechanism

1. Let I_{CT} and I_{MRI} are the two source images considered for fusion

2. Each of the source images are subjected to CLAHE operation to get contrast-enhanced images, which are still labeled as I_{CT} and I_{MRI}

3. Each of the source images from step 2 are applied for multi scale and multi directional decomposition using NSCT to provide respective base layers B_{CT} and B_{MRI} and detail layers D_{CT} and D_{MRI} and detail layers

4. Compute energy of each base layer using equation (5) to give $E_{CT}(x,y)$ and $E_{MRI}(x,y)$

5. From the energy information, compute weight maps of base layers as follows:

$$W_{CT}(x,y) = \frac{E_{CT}(x,y)}{E_{CT}(x,y) + E_{MRI}(x,y)} \quad (7)$$

$$W_{MRI}(x,y) = \frac{E_{MRI}(x,y)}{E_{CT}(x,y)+E_{MRI}(x,y)} \quad (8)$$

6. Generate fused base image using weighted combination of base layers B_{CT} and B_{MRI}

$$B_{fused} = W_{CT}(x,y)B_{CT} + W_{MRI}(x,y)B_{MRI} \quad (9)$$

7. Apply cross guided filter on each detail and compute the fine details of the layers.

$$S_{CT} = guidedfilter(D_{CT}, D_{MRI}, r, \epsilon) \quad (10)$$

$$S_{MRI} = guidedfilter(D_{MRI}, D_{CT}, r, \epsilon) \quad (11)$$

8. Fine details of CT image, $F_{CT} = D_{CT} - S_{CT}$ (12)

9. Fine details of CT image, $F_{MRI} = D_{MRI} - S_{MRI}$ (13)

10. Compute gradient of fine details using equation (6) to give G_{CT} and G_{MRI}

11. From the gradient information, compute weight maps of detail layers as follows:

$$W_1(x,y) = \begin{cases} 1 & if \;\; G_{CT}(x,y) \geq G_{MRI}(x,y) \\ 0 & elsewhere \end{cases} \quad (14)$$

$$W_2(x,y) = 1 - W_1(x,y) \quad (15)$$

12. Generate fused detail layer at each scale and direction using weighted average fusion

$$. D_{\theta,fused} = \frac{W_1(x,y)D_{\theta,CT}+W_2(x,y)D_{\theta,MRI}}{W_1(x,y)+W_2(x,y)} \quad (16)$$

13. Reconstruct the fused image from B_{fused} and $D_{\theta,fused}$ using inverse NSCT

4. Results and discussion

The experiments were conducted using multiple pairs of medical datasets to assess the effectiveness of the proposed method. However, for this study, only three pairs of CT-MRI medical datasets have been considered and presented, as illustrated in Fig. 3. These datasets are labeled as Dataset1, Dataset2, and Dataset3, respectively.These are the benchmark images collected from https://www.med.harvard.edu/AANLIB/home.html. To evaluate the performance and validity of the proposed method, three key fusion evaluation metrics are considered: Fusion Information Score (QAB/F), Fusion Loss (LAB/F), and Fusion Artifacts (NAB/F). These widely used metrics provide a comprehensive analysis of fusion efficiency. QAB/F measures the total information transferred from the input images to the fused image, ensuring effective fusion. LAB/F quantifies the cumulative loss of information during the fusion process, while NAB/F assesses the noise or artifacts introduced due to the fusion operation. For an optimal fused image, QAB/F should have a high value, indicating better information retention, whereas LAB/F and NAB/F should be minimal to ensure minimal information loss and artifact introduction.

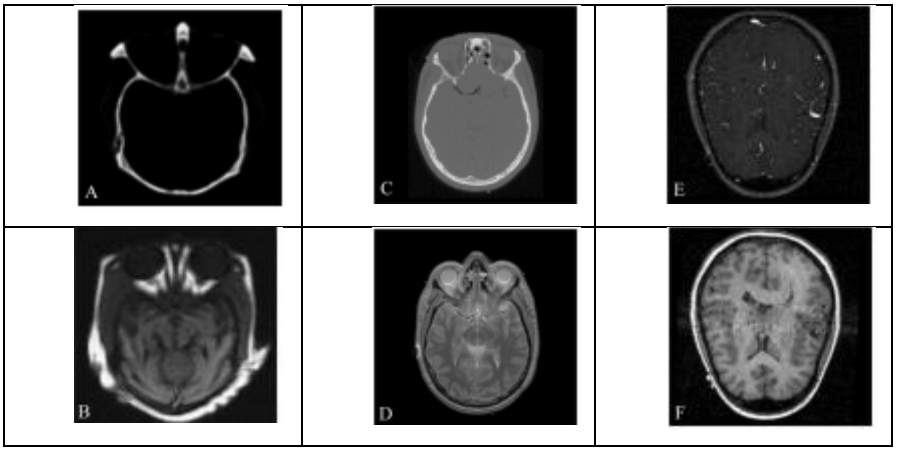

Figure 3: Datasets used for evaluation: Dataset 1(A and B), Dataset 2(C and D), Dataset 3(E and F)

If A and B are input images and F is the fused image then the weighted sum of edge details quantified from both source images, denoted as QAF and QBF, is used to assess the overall fusion performance QAB/F. In this evaluation, the weight parameters W**A** and WB represent the perceptual significance of each pixel in the source images. The value of QAB/F ranges between 0 and 1, where 0 indicates complete loss of source information, while QAB/F = 1 signifies an ideal fusion with no loss of input information. The perceptual weights W**A** and WB are assigned based on the respective gradient strength factors G**A** and GB, providing a simple yet effective method to incorporate edge details in the fusion process.

$$Q_{AB/F} = \frac{\sum_{\forall n,m} Q^{AF}_{n,m} W^{A}_{n,m} + Q^{BF}_{n,m} W^{B}_{n,m}}{\sum_{\forall n,m} W^{A}_{n,m} + W^{B}_{n,m}} \quad (17)$$

$$\text{Fusion loss, } L_{AB/F} = \frac{\sum_{\forall n,m} r_{n,m}([1-Q^{AF}_{n,m}) W^{A}_{n,m} + (1-Q^{BF}_{n,m}) W^{B}_{n,m}}{\sum_{\forall n,m} W^{A}_{n,m} + W^{B}_{n,m}} \quad (18)$$

$$r_{n,m} = \begin{cases} 1 & if \;\; g^F_{n,m} < \;\; g^A_{n,m} \; or \; g^F_{n,m} < \;\; g^B_{n,m} \\ 0 & elsewhere \end{cases} \quad (19)$$

$$N_{n,m} = \begin{cases} 2 - \mathrm{Q}^{\mathrm{AF}}_{\mathrm{n,m}} - \mathrm{Q}^{\mathrm{BF}}_{\mathrm{n,m}} & if \;\; g^F_{n,m} > \;\; g^A_{n,m} \; and \;\; g^B_{n,m} \\ 0 & elsewhere \end{cases} \quad (20)$$

Fusion artifacts, $N_{AB}/_F = \frac{\sum_{\forall n,m} N_{n,m}(\mathrm{W}^{\mathrm{A}}_{\mathrm{n,m}} + \mathrm{W}^{\mathrm{B}}_{\mathrm{n,m}})}{\sum_{\forall n,m} \mathrm{W}^{\mathrm{A}}_{\mathrm{n,m}} + \mathrm{W}^{\mathrm{B}}_{\mathrm{n,m}}}$ (21)

The fusion loss (LAB/F) quantifies the amount of detail lost during the fusion process. When QAF and QBF are less than 1, it directly indicates a loss of information from the source images. However, to accurately evaluate fusion loss, it is crucial to differentiate it from fusion artifacts, which may also lead to QAF and QBF < 1. The QAB/F approach utilizes gradient strength to compare the input and fused images. A fused image F is classified as containing artifacts if its gradient strength exceeds that of the input images. Conversely, if the gradient strength in F is weaker than in the inputs, it implies a loss of details. The total fusion loss is then computed as the perceptually weighted local fusion loss, represented by 1 − QAF and 1 − QBF for input images A and B, respectively.

Fusion artifacts NAB/F refer to visual details introduced into the fused image during the fusion process that do not correspond to any features present in the input images. These artifacts are essentially erroneous data that can reduce the effectiveness of the fused image and may significantly impact certain fusion applications. Fusion artifacts can be analyzed using the adopted framework by identifying gradient details that appear in the fused image but are absent in both source images. A local estimate of fusion artifacts, often referred to as fusion noise ($N_{n,m}$), is computed as the fusion loss in regions where the fusion gradients are stronger than those in the input images.

4.1 Qualitative analysis

The brain datasets presented in Figure 3 are obtained using CT and MRI modalities. As mentioned earlier, CT images effectively capture bone structures and hard tissues, whereas MRI images provide detailed visualization of soft tissues in the brain. Therefore, the fusion process plays a crucial role in integrating complementary information from both modalities into a single image, ensuring comprehensive visualization for accurate diagnosis and treatment planning. Figure 4 presents the visual results of various fusion techniques applied to Dataset1, demonstrating the effectiveness of the proposed fusion method in preserving essential anatomical details.

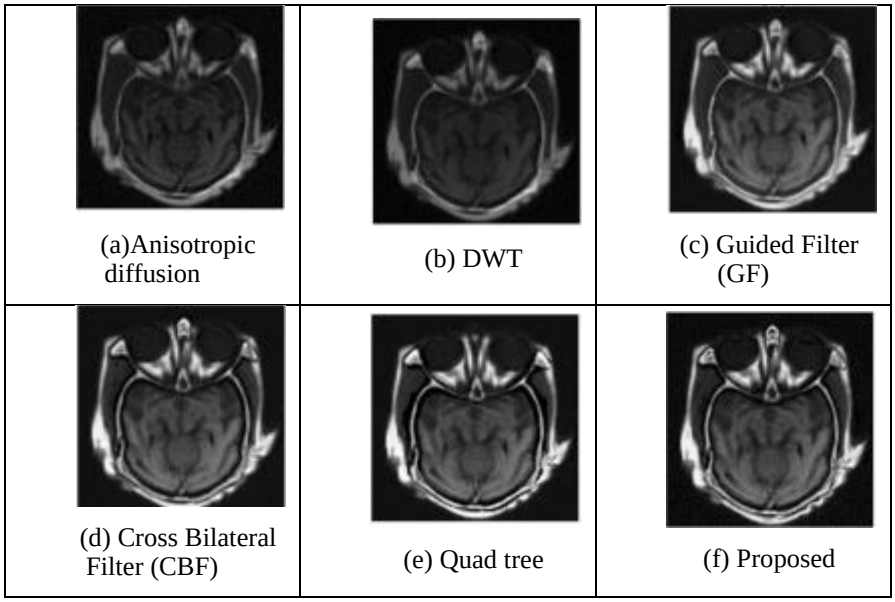

(a)Anisotropic diffusion | (b) DWT | (c) Guided Filter (GF)

(d) Cross Bilateral Filter (CBF) | (e) Quad tree | (f) Proposed

Figure 4: Fusion results of Dataset 1

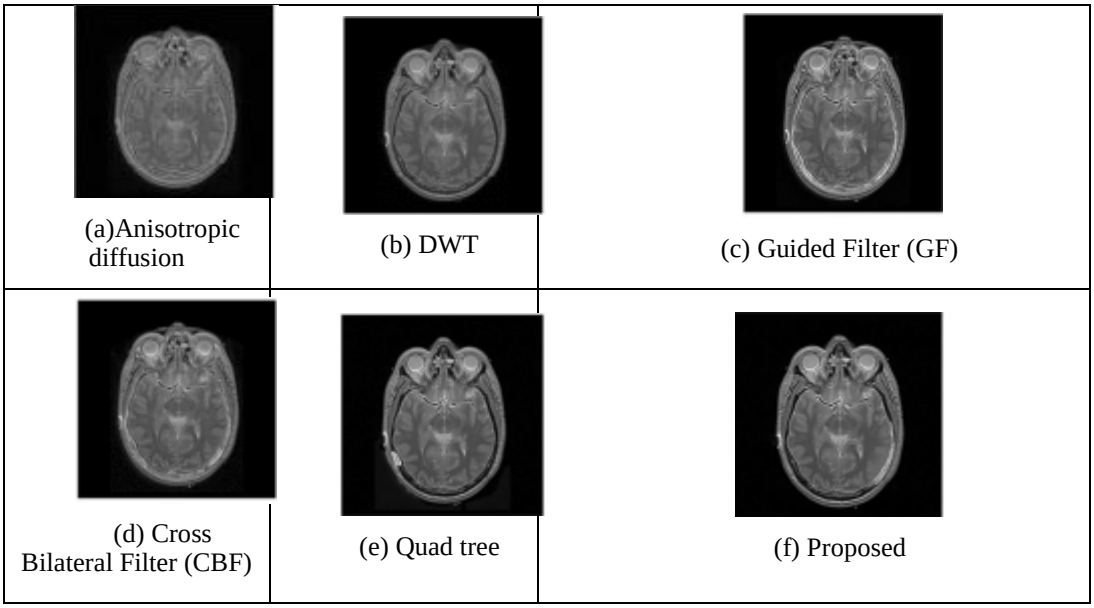

Figure 5: Fusion results of Dataset 2

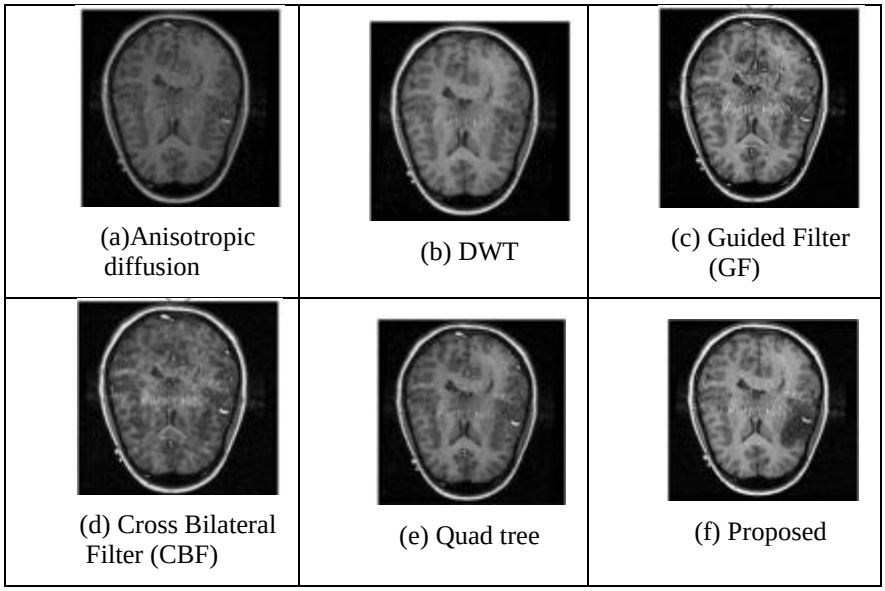

Figure 6: Fusion results of Dataset 3

Figure 4a–f presents the fused images obtained using various fusion algorithms, while Figure 3f demonstrates the fused image produced by our proposed method. The results indicate that the fused images generated using the Anisotropic Diffusion and DWT methods exhibit noticeable visual distortions and lack sufficient contrast, making them less effective. Through visual analysis, the fusion results of GF, CBF, and the Quadtree method appear visually better. However, in comparison to these methods, the proposed approach produces a more visually enhanced and undistorted fused image, effectively preserving essential structural and textural details from both CT and MRI images. The results of Dataset 2, depicted in Figure 5, indicate that the anisotropic diffusion method suffers from noticeable detail loss and poor fusion performance. The DWT and GF methods effectively integrate essential information, generating visually appealing results. The CBF and Quadtree methods further enhance the object region and improve the contrast between the object and background; however, the background resolution remains insignificant. In comparison to these techniques, the fused image obtained using the proposed method retains more visual details, ensuring better clarity and structural preservation.

Figure 6 presents the visual results of different fusion techniques for Dataset 3. The Guided Filter, Anisotropic Diffusion, and DWT algorithms struggle to effectively combine all complementary information from the paired source images. The Quadtree and CBF algorithms manage to retain essential details and produce visually appealing results. However, in comparison to other methods, the fusion result of the proposed approach delivers superior visual quality, preserving more information with enhanced contrast. Across all datasets, the fused images generated by the proposed algorithm exhibit better visual performance and comparable quantitative values compared to existing techniques. Additionally, experimental results on different image sets confirm that the proposed method has a faster runtime than various traditional benchmark fusion algorithms.

4.2 Quantitative analysis

Our method is quantitatively analyzed in contrast to different fusion methods using the fusion metrics $Q_{AB/F}$, $L_{AB/F}$ and $N_{AB/F}$. During the fusion process, $Q_{AB/F}$ indicates total information transfers from input images into fused image, $L_{AB/F}$ indicates total information loss and $N_{AB/F}$ indicates noise or artifacts added during fusion process. Any method should have higher value for $Q_{AB/F}$ and minimal values in case of $L_{AB/F}$ and $N_{AB/F}$ for better performance. Table 1 demonstrates the quantitative performance of different image fusion techniques as well as the proposed algorithm for all three image datasets.

Table 1: Quantitative results several medical image datasets

Method	Dataset 1			Dataset 2			Dataset 3		
	$Q_{AB/F}$	$L_{AB/F}$	$N_{AB/F}$	$Q_{AB/F}$	$L_{AB/F}$	$N_{AB/F}$	$Q_{AB/F}$	$L_{AB/F}$	$N_{AB/F}$
Anisotropic diffusion	0.659	0.339	0.002	0.687	0.310	0.003	0.817	0.182	0.001
DWT	0.624	0.376	0.000	0.780	0.220	0.000	0.835	0.165	0.000
GF	0.862	0.137	0.001	0.763	0.236	0.001	0.859	0.135	0.006
CBF	0.883	0.106	0.011	0.754	0.243	0.033	0.848	0.127	0.025
Quadtree	0.906	0.082	0.012	0.805	0.193	0.002	0.843	0.151	0.006
Proposed	0.915	0.077	0.008	0.824	0.175	0.001	0.883	0.114	0.003

The proposed method achieves the highest $Q_{AB/F}$ scores across all datasets (0.915, 0.824, and 0.883), demonstrating superior information retention. Quadtree and CBF methods also show good performance, particularly in Dataset 1, but fall short in other datasets. In contrast, anisotropic diffusion and DWT exhibit relatively lower $Q_{AB/F}$ scores, suggesting they fail to preserve crucial information effectively. Fusion loss ($L_{AB/F}$) measures the amount of information discarded during the fusion process, where lower values indicate better retention of source image details. The proposed method outperforms all other techniques by achieving the lowest $L_{AB/F}$ values across all datasets (0.077, 0.175, and 0.114), indicating minimal loss of important image features. Quadtree and CBF methods also perform reasonably well, particularly in Dataset 1, but show slightly higher fusion loss in other datasets. On the other hand, DWT and anisotropic diffusion methods suffer from higher fusion loss, especially in Dataset 1 (0.376 and 0.339, respectively), confirming their limitations in retaining essential image details.

Fusion artifacts ($N_{AB/F}$) represent unwanted distortions or noise introduced during the fusion process. Lower $N_{AB/F}$ values indicate fewer visual inconsistencies in the fused image. The proposed method achieves near-zero $N_{AB/F}$ scores across all datasets (0.008, 0.001, and 0.003), confirming its ability to generate high-quality fused images with minimal distortions. DWT consistently produces zero or near-zero $N_{AB/F}$ values, indicating that it minimizes noise but might also lose finer details. However, CBF and Quadtree methods introduce slightly higher artifacts, particularly in Dataset 2 (0.033 and 0.002, respectively), which may negatively impact fusion quality. Overall, the proposed method demonstrates the best fusion performance by achieving the highest information retention ($Q_{AB/F}$), the lowest information loss ($L_{AB/F}$), and minimal artifacts ($N_{AB/F}$). While Quadtree and CBF methods also perform well, they introduce slightly higher fusion loss or artifacts in some cases. In contrast, DWT and anisotropic diffusion methods exhibit weaker performance, with lower information retention and higher loss. The results confirm that the proposed fusion technique is highly effective in medical image fusion, providing visually superior and quantitatively optimal results across all datasets.

5. Conclusion

The proposed fusion method demonstrates significant improvements across all datasets in terms of information retention, fusion loss reduction, and artifact minimization.

The experimental results show that the proposed method effectively preserves relevant details from source images while minimizing unwanted distortions and loss of critical information. In terms of information retention ($Q_{AB/F}$), the proposed method achieves a minimum improvement of 5.75% and a maximum improvement of 38.23% compared to existing fusion techniques. The reduction in fusion loss ($L_{AB/F}$) ranges from a minimum of 6.09% to a maximum of 79.52%, indicating better preservation of structural details. Additionally, the suppression of fusion artifacts ($N_{AB/F}$) shows improvements ranging from 10.00% to 96.97%, ensuring that the fused images maintain high visual quality without introducing unnecessary distortions. Overall, the proposed method provides a balanced fusion approach that enhances visual clarity, improves diagnostic reliability, and ensures minimal information loss. The results confirm its effectiveness in medical image fusion, making it a strong candidate for clinical applications where accurate and high-quality image representation is essential.

References

[1] S. Y. Kim, M. Beer, and D. W. T. Vogel, “Imaging in head and neck cancers: Update for non-radiologist,” Van Medical Journal, vol. 120, p.105434, 2021.

[2] Kim GU, Park WT, Chang MC, Lee GW, “Diagnostic Technology for Spine Patholog,” Asian Spine , vol. 16,no.5, p.764-775, Oct 2022.

[3] S. Najeeb and S. Ali, “Finding the discriminative frequencies of motor electroencephalography signal using genetic algorithm,” TELKOMNIKA, vol. 19, no. 1, pp. 285–291, 2021.

[4] Vikrant Bhateja, Aisha Moin, Anuja Srivastava, Le Nguyen Bao, Aimé Lay-Ekuakille, Dac-Nhuong Le, “Multispectral medical image fusion in Contourlet domain for computer based diagnosis of Alzheimer’s disease,” *Rev. Sci. Instrum,* vol. 87, no. 7,July 2016.

[5] Karthikeyan and B. Ramadoss, “Comparative analysis of similarity measure performance for multimodality image fusion using DTCWT and SOFM with various medical image fusion techniques,” Indian Journal of Science Technology, vol. 9, no. 22, pp. 1–6, 2016.

[6] R. M. Al_airaji, I. A. Aljazaery, S. K. Al_dulaimi, and H. T. S. Alrikabi, “Generation of high dynamic range for enhancing the panorama environment,” Bulletin of Electrical Engineering and Informatics, vol. 10, no. 1, pp. 138–147, 2021.

[7] G. Bhatnagar, Q. M. J. Wu and Z. Liu, "Directive Contrast Based Multimodal Medical Image Fusion in NSCT Domain," in IEEE Transactions on Multimedia, vol. 15, no. 5, pp. 1014-1024, Aug. 2013,

[8] L. Cai, J. Gao, and D. Zhao, “A review of the application of deep learning in medical image classification and segmentation,” Annals of translational medicine, vol. 8, no. 11, 2020.

[9] J. Agarwal and S. S. Bedi, “Implementation of hybrid image fusion technique for feature enhancement in medical diagnosis,” Human-centric Computing and Information Sciences, vol. 5, article no. 3, Feb.2015. https://doi.org/10.1186/s13673-014-0020-z

[10] S. Aymaz and C. Kose,“Multi-focus image fusion using stationary wavelet transform (SWT) with principal component analysis (PCA),” Proceedings of 10th International Conference on Electrical and Electronics Engineering (ELECO), Bursa, Turkey, pp. 1176-1180,2017.

[11] D. P. Bavirisetti and R. Dhuli, “Fusion of infrared and visible sensor images based on anisotropic diffusion and Karhunen-Loeve transform,” IEEE Sensors Journal, vol. 16, no. 1, pp. 203-209, Jan.2016.

[12] J. Ma, Z. Zhou, B. Wang, and H. Zong, “Infrared and visible image fusion based on visual saliency map and weighted least square optimization,” Infrared Physics & Technology, vol. 82, pp. 8-17, May.2017.

[13] K. Zhan, Y. Xie, H. Wang, and Y. Min, “Fast filtering image fusion,” Journal of Electronic Imaging, vol. 26, no. 6, Nov. 2017. https://doi.org/10.1117/1.JEI.26.6.063004.

[14] L. Lu, X. Ren, K. H. Yeh, Z. Tan, and J. Chanussot, “Exploring coupled images fusion based on joint tensor decomposition,” Human-centric Computing and Information Sciences, vol. 10, article no. 10, March.2020. https://doi.org/10.1186/s13673-020-00215.

[15] X. Li, X. Guo, P. Han, X. Wang, H. Li, and T. Luo, “Laplacian redecomposition for multimodal medical image fusion,” IEEE Transactions on Instrumentation and Measurement, vol. 69, no. 9, pp. 6880-6890,Sep.2020.

[16] B. Goyal, D. C. Lepcha, A. Dogra, V. Bhateja, and A. Lay-Ekuakille, “Measurement and analysis of multimodal image fusion metrics based on structure awareness using domain transform filtering,” Measurement, vol. 182, article no. 109663,Sep.2021. https://doi.org/10.1016/j.measurement.2021.109663.

[17] J. Jose, N. Gautam, M. Tiwari, T. Tiwari, A. Suresh, V. Sundararaj, and M. R. Rejeesh, “An image quality enhancement scheme employing adolescent identity search algorithm in the NSST domain for multimodal medical image fusion,” Biomedical Signal Processing and Control, vol. 66, article no. 102480,Apr.2021. https://doi.org/10.1016/j.bspc.2021.102480.

[18] M. Kaur and D. Singh,“Multi-modality medical image fusion technique using multi-objective differential evolution based deep neural networks,” Journal of Ambient Intelligence and Humanized Computing, vol. 12, no. 2, pp. 2483-2493,Aug.2020.

[19] MV Srikanth, VVKDV Prasad and K Satya Prasad, “A 2D Histogram-Based Image Thresholding Using Hybrid Algorithms for Brain Image Fusion,” International Journal of

System Dynamics Applications (IJSDA), Volume 11, Issue 6,2022

[20] MV Srikanth, VVKDV Prasad and K Satya Prasad, "An improved firefly algorithm-based 2-D image thresholding for brain image fusion," International Journal of Cognitive Informatics and Natural Intelligence (IJCINI), Volume 14, Issue 3,2020

[21] M. Srikanth, V. Prasad, and K.Satya Prasad, "Brain Tumor Detection Through Modified Optimization Algorithm by Region-based Image Fusion," ECTI-CIT Transactions, vol. 17, no. 1, pp. 117–127,Mar.2023.

[22] M. V. Srikanth, V. V. K. D. V. Prasad, and K. S. Prasad, "Application of Novel Improved Firefly Algorithm for Image Fusion To Detect Brain Tumor, " ECTI-CIT Transactions, vol. 17, no. 2, pp. 292–307, Jun. 2023.

[23] S. M.V., S. Kethavath, S. Yerram, S. Kalli, Nagasirisha.B, and J. Brahmaiah Naik, "Brain Tumor Detection through Image Fusion Using Cross Guided Filter and Convolutional Neural Network", ECTI-CIT Transactions, vol. 18, no. 4, pp. 579–590, Oct. 2024.